ISSN 1028-334X, Doklady Earth Sciences, 2021, Vol. 501, Part 1, pp. 925–932. © Pleiades Publishing, Ltd., 2021.
Russian Text © The Author(s), 2021, published in Doklady Rossiiskoi Akademii Nauk. Nauki o Zemle, 2021, Vol. 501, No. 1, pp. 34–42.

PETROLOGY

Valanginian Subalkaline Magmatism of the Rassokha and Argatass Terranes (Northeastern Russia)

S. N. Sychev[a,b,c,*], O. Yu. Lebedeva[a,b], A. K. Khudoley[a,b], Corresponding Member of the RAS S. D. Sokolov[c], A. V. Rogov[b], V. S. Maklashin[b], and P. A. Lvov[b]

Received May 13, 2021; revised June 7, 2021; accepted June 8, 2021

Abstract—Based on the U–Th–Pb (SIMS) dating of zircons from magmatic bodies of trachytes and trachydolerites of the Upper Agyndzha complex located within the Rassokha island arc and Argatass oceanic terranes, we have reached a conclusion about the Valanginian age of its formation. In terms of the age and composition, the Valanginian volcanics of the Rassokha and Argatass terranes are close to those of the base of the Alazeya–Indigirka zone. The spatial position of Valanginian trachytes and trachydolerites does not allow us to consider them as suprasubduction formations of the Andean-type margin. This is due to the distance of these bodies from the main field of the Alazeya–Indigirka zone. It can be concluded that the formation of these bodies was associated with the extension within this zone. The tectonic position of the Valanginian magmatic bodies allows us to interpret them as complexes that amalgamated two geodynamically different terranes.

Keywords: subalkaline rocks, U–Th–Pb (SIMS) method, Valanginian, Rassokha and Argatass terranes
DOI: 10.1134/S1028334X2109018X

The Rassokha (Rassoshinsky) island arc and Argatass oceanic terranes are located in the western part of the Verkhoyansk–Chukotka Fold Belt, within the Verkhoyansk–Kolyma fold system. These terranes extend in the northwesterly direction bounded on the southwest by the Omulevka terrane of the passive continental margin [1]. The Rassokha terrane is composed of Cambrian–Ordovician and Devonian–Early Jurassic volcanogenic and sedimentary formations; the Argatass terrane is made of Late Paleozoic–Early Mesozoic basalts and schists [2]. The rock complexes of the Rassokha and Argatass terranes are overlain with an angular unconformity by Middle–Late Jurassic volcanics of the Uyandina–Yasachnaya belt (Fig. 1). In the upper reaches of the Agyndzha River and the Rassokha River basin are volcanic bodies cutting Ordovician and Permian rocks. The age of these bodies was previously considered close to the time of formation of the host strata [3, 4]. This work presents new U–Th–Pb (SIMS) ages of zircons, which allowed us to date the trachyte and trachydolerite bodies formed in the post-amalgamation stages of the development of the collage of terranes of northeastern Russia, back to the Early Cretaceous.

The magmatic bodies in the Agyndzha River area were attributed to the Middle–Late Ordovician and Late Silurian formations in the geological maps of the 1980s [3, 4]. We have performed geological mapping within potential gold-copper–porphyry objects in the upper reaches of the Agyndzha River and the Rassokha (Rassoshinsky) granite massif and studied rocks of higher alkalinity to determine their ages and petrological characteristics. The volcanogenic–sedimentary section, intruded by numerous bodies of alkaline rocks of mafic and intermediate composition, is exposed in the Agyndzha River canyon [5]. Based on paleontological finds, the host sedimentary rocks have a Middle–Late Ordovician age [6]. To the east of the Rassokha massif, all the cover formations were previously attributed to the Late Paleozoic [3, 4].

Samples were taken from a subvolcanic trachyte body (sample 3036/9) of about 30 m thick, located in the lower part of the Agyndzha River canyon, near the contact with conglomerates, and from a trachydolerite dike (sample 3038/14) of about 1 m thick, located 400 m upstream from the canyon. The trachyte flows of about 600 m were found on the left side of the Rassokha River, 2.5 km downstream from the mouth of Goticheskii Creek; a sample was taken from the middle part of the nappe (sample 3054/6).

The U–Th–Pb (SIMS) dating of zircons was carried out on a SHRIMP-II secondary ion microprobe

[a] *St. Petersburg State University, St. Petersburg, 199034 Russia*
[b] *A.P. Karpinsky Russian Geological Research Institute, St. Petersburg, 199106 Russia*
[c] *Geological Institute, Russian Academy of Sciences, Moscow, 119017 Russia*
**e-mail: s.sychev@spbu.ru*

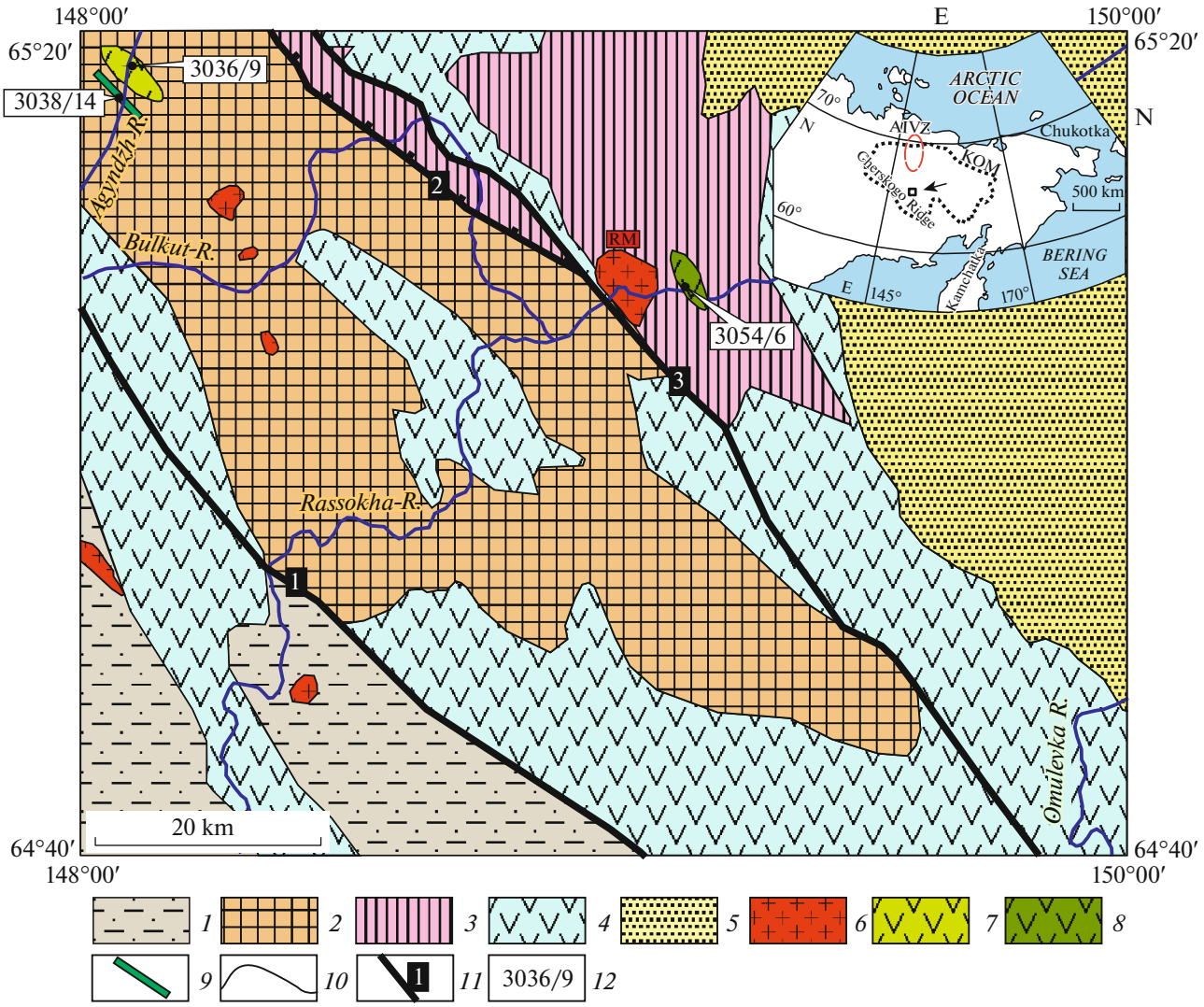

Fig. 1. The distribution of the Valanginian volcanics within the Rassokha and Argatass terrane on the tectonic map (modified after [4]). (*1*–*5*) Regional subdivisions: (*1*) Omulevka terrane (Middle Ordovician–Lower Carboniferous terrigenous–carbonate deposits), (*2*) Rassokha terrane (Cambrian–Ordovician and Devonian–Jurassic volcanogenic and sedimentary deposits), (*3*) Argatass terrane (Upper Paleozoic deep-water basalts and shales and Devonian paleo-rift formations), (*4*) Uyandina–Yasachnaya volcanic belt (Middle–Upper Jurassic volcanics), (*5*) Ozhogino depression (Paleogene–Neogene sedimentary deposits); (*6*–*9*) magmatic formations: (*6*) granitoid massifs, (*7*) subvolcanic bodies of trachytes and trachydacites, (*8*) trachyte flows, (*9*) trachydolerite and dolerite dikes, (*10*) geological boundaries, (*11*) regional faults and their numbers ((1) Garmychan fault, (2) Bulkut thrust, (3) Argatass fault), (*12*) sampling sites and their numbers. KOM, Kolyma–Omolon microcontinent, AIVZ, Alazeya–Indigirka volcanic zone, and RM, Rassokha (Rassoshinskii) massif.

at the Centre of Isotopic Research (CIR) A.P. Karpinsky Russian Geological Research Institute (VSEGEI).

The manually selected zircon grains were mounted in the epoxy resin together with the TEMORA and 91 500 zircon standards and polished to about half of their thickness.

The optical (in transmitted and reflected light) and cathodoluminescent images reflecting the internal structure and zoning of zircons were used to select the measurement points on the zircon surface.

Measurements of the U–Th–Pb ratios on a SHRIMP-II secondary ion microprobe were carried out following the method described in [7]. The intensity of the primary beam of molecular negatively charged oxygen ions was 4 nA, and the diameter of the spot (crater) was 18 μm. The SQUID software was applied for data processing. The U–Th–Pb ratios were normalized to a value of 0.0668 for $^{206}Pb/^{238}U$ ratio of the TEMORA standard zircon, corresponding to an age of 416.75 Ma [8]. The errors of individual analyses (ratios and ages) are at the level of 1σ; the errors of calculated concordant ages and intersects with concordia are at the level of 2σ. The concordia

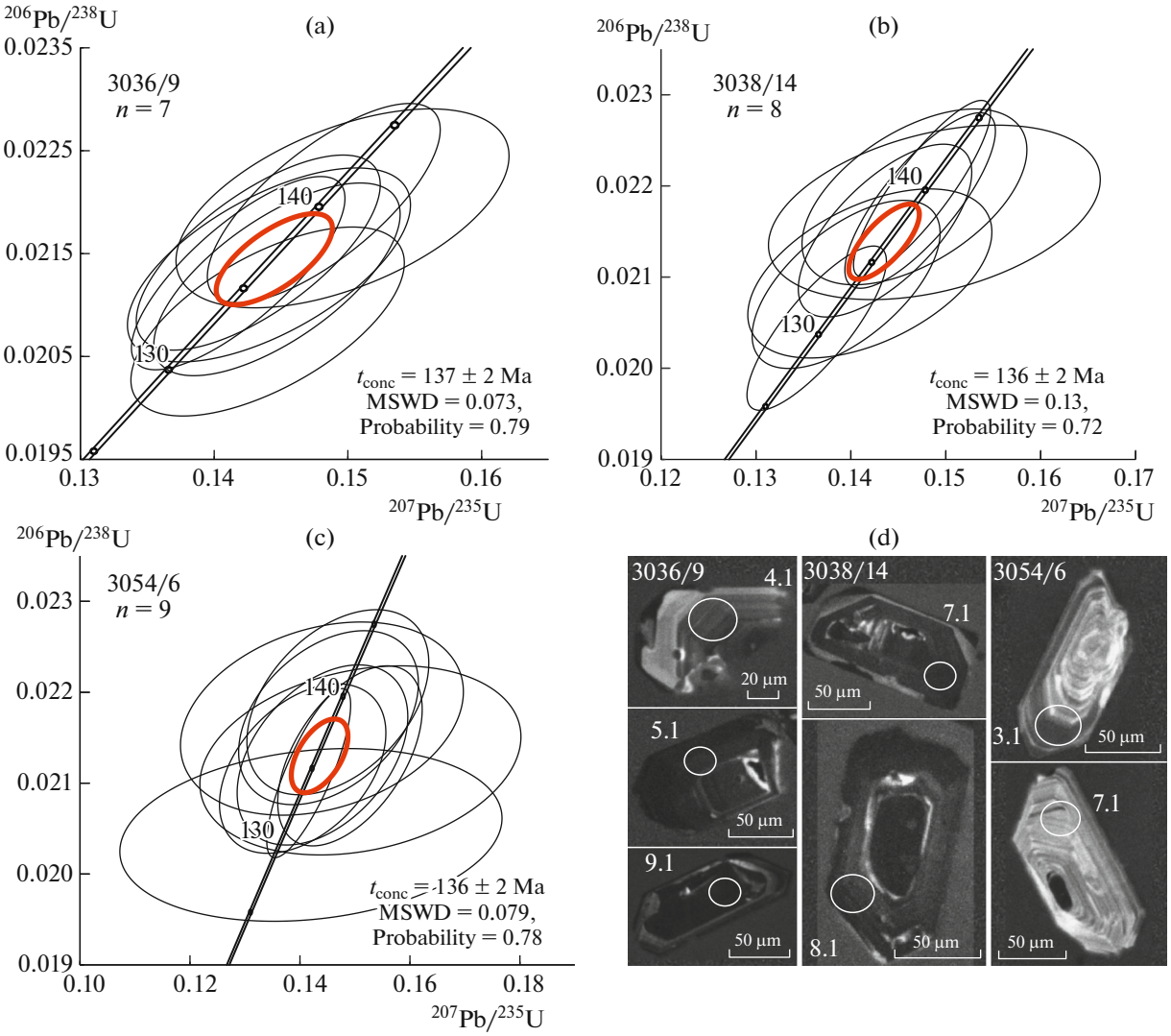

Fig. 2. Concordia diagrams and the morphology of zircon grains. (a) Subvolcanic trachyte body, (b) trachydolerite dike, (c) trachyte flow, and (d) zircons from magmatic bodies with measurement points; the numbers of points correspond to those in Table 1.

diagrams were constructed using the ISOPLOT/EX software.

The results are shown in Fig. 2 and Table 1.

The studies on a CamScan MX 2500S electron microscope revealed that most zircon crystals have a subidiomorphic habit, often with well-preserved faces. The oscillatory zoning characteristic of magmatic zircons is clearly visible in CL images, although individual grains have a more complex structure (Fig. 2d). The high Th/U values (0.42–1.67) in the studied zircons also indicate in favor of the magmatic origin (Table 1). Metamorphic rims are not observed.

Zircons from samples 3036/9 and 3038/14 (Agyndzha River basin) yielded concordant ages of 137 ± 2 and 136 ± 2 Ma, respectively. A concordant age of 136 ± 2 Ma was obtained for sample 3054/6 (Rassokha River basin). All three dates fit into a short period corresponding to the Valanginian stage of the Early Cretaceous.

Chemical analyses of 20 samples were performed in the Central Laboratory at A.P. Karpinsky Russian Geological Research Institute (St. Petersburg). The results obtained are shown in Table 2 and Fig. 3. According to the chemical composition, the rocks are classified as trachytes, trachydacites, pantellerites, trachyrhyodacites, trachybasalts, and basalts (Fig. 3a). The bodies of subalkaline composition are divided into two groups on the Ta/Yb–Th/Yb discriminant diagram [10]. Dolerites and trachydolerites lie in the fields of rocks of the calc-alkaline and tholeiitic series; trachytes lie in the distribution field of the calc-alkaline magma series of the active continental margins (Fig. 3b). According to the fractionated REE distribution demonstrating enrichment in LREEs and depletion in HREEs (Fig. 3c), as well as the presence of

Table 1. Results of U–Th–Pb (SIMS) study of zircons from igneous rocks of the Rossokha and Argatass terranes

Point	$^{206}Pb_c$, %	U, ppm	Th, ppm	$^{206}Pb^*$, ppm	$^{206}Pb/^{238}U$, Ma		$^{207}Pb/^{206}Pb$, Ma		$^{207}Pb^*/^{206}Pb^*$	±%	$^{207}Pb^*/^{235}U$	±%	$^{206}Pb^*/^{238}U$	±%	Rho
Subvolcanic body of trachytes, Sample 3036/9 (65°19′6.6″ N, 148°3′47.4″ E)															
1.1	0.17	1565	1574	28.1	133	±2	200	±53	0.0501	2.3	0.14	2.9	0.0208	1.8	0.6
2.1	0.12	2139	1974	39.1	136	±2	166	±46	0.0494	2	0.14	2.6	0.0213	1.8	0.7
3.1	0.00	2518	2716	46.1	136	±2	112	±34	0.0483	1.5	0.14	2.3	0.0213	1.8	0.8
4.1	0.00	964	889	17.7	136	±3	142	±55	0.0489	2.3	0.14	3	0.0214	1.8	0.6
5.1	0.14	2525	3303	46.7	137	±2	115	±43	0.0483	1.8	0.14	2.6	0.0215	1.8	0.7
6.1	0.41	2942	2175	55.7	140	±3	170	±68	0.0495	2.9	0.15	3.4	0.0219	1.8	0.5
7.1	0.26	4111	5502	77.9	140	±3	142	±38	0.0489	1.6	0.15	2.4	0.0220	1.8	0.7
8.1	0.00	5946	6985	113	141	±3	110	±22	0.0482	0.9	0.15	2	0.0221	1.8	0.9
9.1	0.51	7658	3308	159	153	±3	156	±44	0.0492	1.9	0.16	2.6	0.0240	1.8	0.7
10.1	2.14	7028	5263	152	157	±3	144	±110	0.0489	4.7	0.17	5.1	0.0247	1.8	0.4
11.1	0.30	5380	5014	116	160	±3	183	±43	0.0497	1.8	0.17	2.6	0.0251	1.8	0.7
Trachydolerite dike, Sample 3038/14 (65°18′51.9″ N, 148°2′50.4″ E)															
1.1	0.03	3331	4405	58.5	131	±2	119	±30	0.0484	1.3	0.14	2.2	0.0204	1.8	0.8
2.1	0.68	3315	4526	60	133	±2	118	±54	0.0484	2.3	0.14	2.9	0.0209	1.8	0.6
3.1	0.78	2374	2524	43.2	134	±2	145	±75	0.0489	3.2	0.14	3.7	0.0210	1.8	0.5
4.1	0.43	3747	3858	69.6	137	±2	119	±46	0.0484	1.9	0.14	2.6	0.0215	1.8	0.7
5.1	0.03	5637	9407	105	138	±2	139	±22	0.0488	0.9	0.15	2	0.0217	1.8	0.9
6.1	1.15	1950	2377	36.8	138	±3	183	±100	0.0497	4.5	0.15	4.8	0.0217	1.8	0.4
7.1	0.14	3789	5507	71.2	139	±2	145	±32	0.0489	1.4	0.15	2.2	0.0218	1.8	0.8
8.1	1.06	3431	2922	65.2	140	±3	130	±66	0.0486	2.8	0.15	3.3	0.0219	1.8	0.5
9.1	0.02	4480	5815	84.6	140	±2	133	±24	0.0487	1	0.15	2	0.0220	1.8	0.9
10.1	0.00	4662	4883	89.7	143	±3	76	±26	0.0475	1.1	0.15	2.1	0.0224	1.8	0.9
11.1	0.02	7946	9931	156	146	±3	125	±18	0.0485	0.8	0.15	1.9	0.0229	1.8	0.9
12.1	0.63	11059	12302	229	153	±3	139	±35	0.0488	1.5	0.16	2.3	0.0239	1.8	0.8
Trachyte flow, Sample 3054/6 (65°7′41.7″ N, 149°8′16.8″ E)															
1.1	1.18	718	420	12.8	130	±3	215	±230	0.0504	9.8	0.14	10	0.0204	1.9	0.2
2.1	0.05	3387	2489	61.5	135	±2	131	±31	0.0487	1.3	0.14	2.2	0.0211	1.8	0.8
3.1	0.38	939	566	17.1	135	±3	107	±94	0.0481	4	0.14	4.4	0.0212	1.8	0.4
4.1	0.61	400	169	7.34	136	±3	260	±180	0.0514	7.6	0.15	7.9	0.0213	2	0.3
5.1	0.18	729	428	13.4	136	±3	230	±71	0.0508	3.1	0.15	3.6	0.0213	1.9	0.5
6.1	0.32	767	374	14.1	136	±3	150	±93	0.0490	4	0.14	4.4	0.0213	1.9	0.4
7.1	0.62	398	172	7.46	139	±3	103	±170	0.0481	7	0.14	7.3	0.0217	2	0.3
8.1	0.57	1306	1210	24.5	139	±3	124	±100	0.0485	4.3	0.15	4.6	0.0217	1.8	0.4
9.1	0.29	572	305	10.8	140	±3	132	±97	0.0487	4.1	0.15	4.6	0.0219	1.9	0.4
10.1	0.56	9327	10857	184	146	±3	92	±32	0.0479	1.3	0.15	2.2	0.0229	1.8	0.8

Pb_c and Pb*, nonradiogenic and radiogenic Pb, respectively. Isotope ratios were ^{204}Pb corrected. The concordia age is calculated based on measurement points 1.1–7.1 (Fig. 2a), 1.1–4.1 and 6.1–9.1 (Fig. 2b), and 1.1–9.1 (Fig. 2c). The calculation of the concordia age is possible only if the following measurements are excluded: 8.1–11.1 for sample 3036/9; 5.1, 10.1–12 for 3038/14; and 10.1 for 3054/6. In accordance with [9], the analyses with U > 5000 ppm were excluded from consideration.

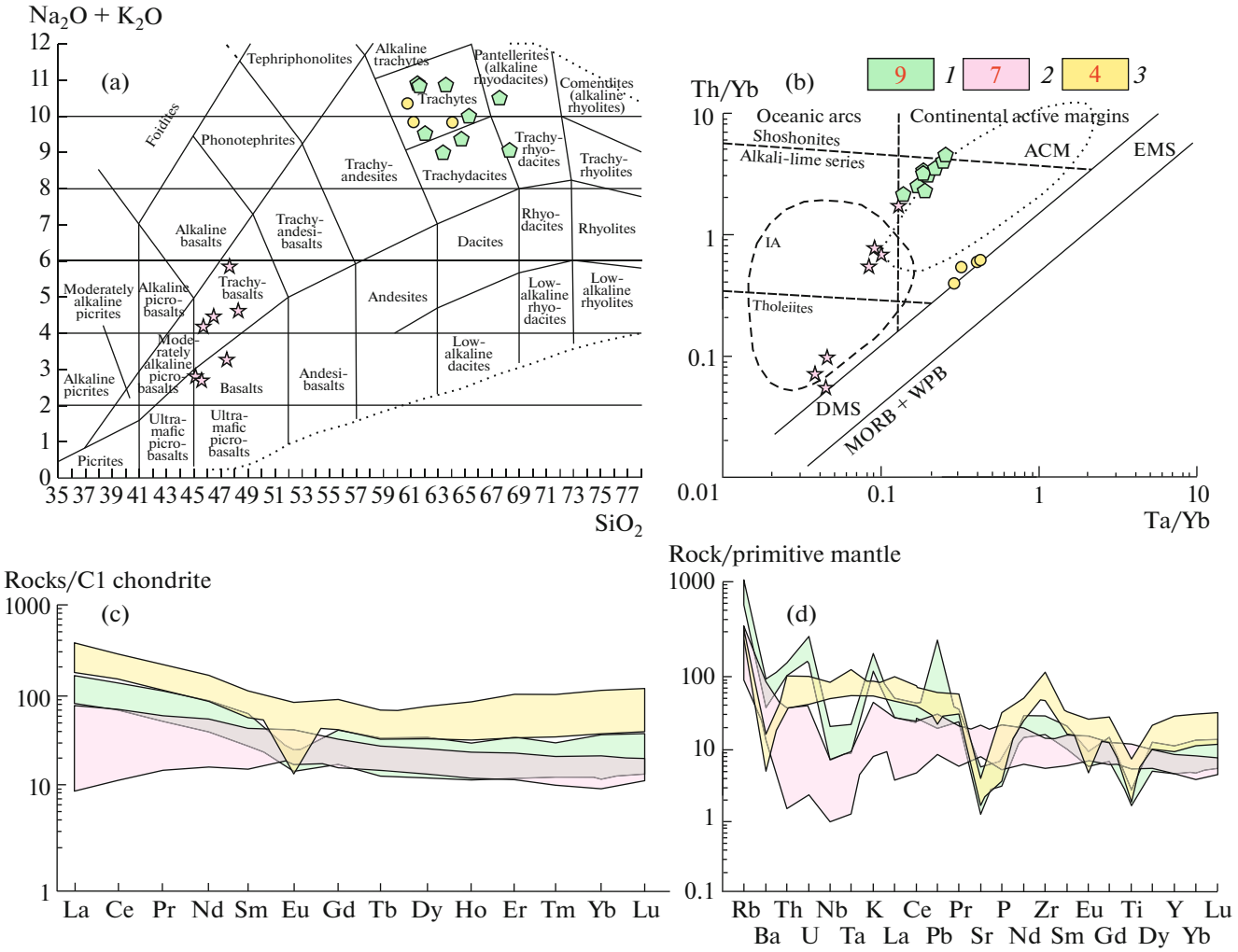

Fig. 3. Geochemical characteristics of volcanic bodies of trachytes, trachydacites, trachydolerites, and dolerites: (*1*) subvolcanic bodies of trachytes and trachydacites in the Agyndzha River basin, (*2*) dike bodies of trachydolerites and dolerites in the Agyndzha River basin, (*3*) a trachyte flow in the Rassokha River basin. Red numerals show the number of analyses. (a) TAS classification diagram, (b) Th/Yb–Ta/Yb diagram [10]. Fields in the diagram show the compositions of igneous rocks, formed in the settings of an island arc (IA) and the active margins of continents (ACM) (after [13]), DMS, depleted mantle; EMS, enriched mantle; MORB+WPB, nonsubduction settings, (c) chondrite-normalized REE distribution, (d) spidergrams. The compositions of C1-chondrite and the primitive mantle are given after [14].

well-pronounced positive K and Pb and negative Ba, Sr, Nb, Ta, Ti, and Eu anomalies (Fig. 3d), they are comparable with rocks of marginal continental suprasubduction environments (for example, volcanics of the Okhotsk–Chukotka volcanic belt [11]). At the same time, similar geochemical characteristics were also established when studying volcanic rocks formed in the setting of extension (rifting) at the rear of the Okhotsk–Chukotka volcanic belt [12].

In terms of composition, the Early Cretaceous volcanics of the Rassokha and Argatass terranes are close to those in the Alazeya–Indigirka zone, with the Nelkan Formation at the base [15]. The effusive rocks of the lower part of the Nelkan Formation section correspond to the calc-alkaline series. They are considered an age analogue of the Berriasian–Barremian Ozhogino Formation [15]. The obtained Valanginian age of the rocks that amalgamated the above-described terranes fit well into the interval of the onset of formation of the Alazeya–Indigirka volcanic zone. The problem is that subalkaline bodies are at a distance from the main field of volcanics of the Alazeya–Indigirka zone. This does not allow us to consider them as Andean-type suprasubduction formations. It is possible that their formation was associated with the development of a volcanic belt, but the formation of the magmatic bodies studied took place in a rifting environment at the rear of the Alazeya–Indigirka volcanic zone, similar to those described in [12]. In the area studied, extension deformations of Early Cretaceous age are noted at the late stages of formation [16]. The low-temperature thermochronological data obtained for

Table 2. Contents of the main (wt %) and trace (ppm) elements in rocks of subvolcanic bodies in the Agyndzha River basin are shown in green, dike bodies in the Agyndzha River basin are in pink, and flows in the Rassokha River basin is in yellow

Sample	SiO_2	TiO_2	Al_2O_3	Fe_2O_3	MnO	MgO	CaO	Na_2O	K_2O	P_2O_5	LOI	Total
3036/9	61.9	0.63	16.2	5.2	0.02	2.42	0.75	2.8	8.08	0.14	1.83	99.9
3044/16	65.2	0.58	16	3.8	0.05	0.98	1.34	3	6.96	0.11	2.3	100
3042/2	63.7	0.48	15.7	3.9	0.05	1.54	0.93	2.9	7.95	0.13	2.54	99.7
3036/12	68.8	0.45	11.4	3.32	0.13	1.39	2.07	1.4	7.37	0.1	3.18	99.7
1035/2	61.9	0.52	16	4.15	0.08	1.18	2.01	0.6	10.2	0.17	3.09	99.9
1036/1	67.9	0.54	16.5	2.01	<.01	0.37	0.1	1.6	9.09	0.06	2.1	100
3039/10	64.8	0.56	16.3	4.09	0.03	1.29	0.99	2.8	6.61	0.17	2.07	99.7
3039/4	63.5	0.51	15.4	4.83	0.1	1	2.22	2.7	6.25	0.15	3.39	100
3039/20	62.4	0.46	14.5	6.15	<.01	1.21	1.28	0.3	9.15	0.14	4.42	100
3038/14	45.6	1.37	16.6	10.1	0.18	8.99	9.19	2.3	1.81	0.11	3.2	99.5
3045/3	46.1	1.66	16.5	10.9	0.21	8.24	8.95	2.6	1.76	0.16	2.53	99.6
75/1	48.4	2.39	15.2	12.7	0.23	5.88	7.75	3.9	0.91	0.35	1.97	99.8
3039/2	45.4	1.54	15.8	10.6	0.18	8.29	9.62	2.4	0.35	0.21	5.27	99.6
3038/13	44.9	1.14	16.5	9.31	0.16	7.53	10.2	2	0.86	0.23	7.21	100
3036/2	47.2	2.54	14.8	12.4	0.23	5.6	8.55	3.6	2.09	0.47	1.65	99
3041/1	48.6	2.06	16	11	0.13	4.94	8.24	2.9	0.56	0.33	5.06	99.9
3054/4	60.8	1.04	16.9	6.75	0.21	0.85	1.91	6.5	3.71	0.24	0.98	99.9
3054/6	60.9	1.43	16.5	5.75	0.13	1.28	2.44	7.2	2.62	0.62	1.02	100
3054/7	73	0.38	11.4	5.1	0.14	0.88	0.92	4	3.25	0.08	0.82	100
3054/2	64	0.73	16.3	5.27	0.13	0.84	1.76	7.3	2.54	0.15	0.71	99.8

Sample	Sc	V	Cr	Co	Ni	Rb	Sr	Y	Zr	Hf	Nb	Ta	Ba	Pb	Th
3036/9	11.9	6.1	3.13	5.28	1.8	110	86.4	42	286	7.2	12	1	512	8	12.7
3044/16	12.6	7.6	7.96	2.19	4	121	79.7	51	334	9.5	15	0.9	260	9	14.1
3042/2	10.4	17.1	7.6	4.05	3.2	149	90.7	35	269	7.7	12	0.8	622	26.2	13.6
3036/12	8.9	5.9	6.46	3.92	4.3	95.3	50.6	33	206	6	9	0.6	668	3.6	9.4
1035/2	12.8	24.6	3.09	2.72	4.3	155	55.7	34	266	7	12	0.8	537	15.7	13.4
1036/1	10.2	22.2	1.78	<0.5	<1.0	162	51.9	23	277	7.8	12	0.8	674	24.2	12.3
3039/10	12.4	24.1	4.38	3.27	4.2	137	48.9	38	282	8.2	13	0.9	478	6.7	14.3
3039/4	12.7	23.6	3.38	1.77	2	109	118	33	275	6.6	11	0.9	472	13.8	14.1
3039/20	8.7	15.8	5.35	16.9	17.3	103	25.1	21	225	6.2	10	0.6	323	31.4	11.2
3038/14	36.4	197	306	47.6	158	34.3	162	24	61	2.1	1	0.1	98.8	1.5	0.1
3045/3	37.4	231	252	45.3	118	45.2	292	28	102	2.8	1	0.1	143	2.3	0.2
75/1	44.9	322	119	40	36.1	14.5	356	38	156	4.4	5	0.4	429	4	3.1
3039/2	33.1	218	292	44	158	5.9	228	30	96	3	3	0.1	127	2.7	0.3
3038/13	28.9	191	210	38.5	127	12.9	406	20	97.5	2.6	4	0.2	261	3.6	3.1
3036/2	40	286	104	35.8	44.7	29.1	374	38	144	3.8	5	0.4	600	5.9	2.5
3041/1	38.8	304	112	29.2	32.4	9.4	449	34	135	3.7	4	0.3	277	4.2	1.9
3054/4	11.1	10	7.87	2.89	8.9	23.8	36.1	70	864	17.5	53	3.4	108	4.4	4.9
3054/6	12.4	5.1	3.63	1.26	4.2	27.8	72.8	92	537	11.4	43	2.4	67.5	10.4	3.1
3054/7	3.4	<2.5	6.51	0.79	2.4	28.4	39.1	131	1220	27.5	56	4.9	32.1	4.1	8.4
3054/2	8.5	9	9.92	2.52	6	17.5	33.2	41	611	12.1	37	2.3	86.8	5	3.4

Table 2. (Contd.)

Sample	U	La	Ce	Pr	Nd	Sm	Eu	Gd	Tb	Dy	Ho	Er	Tm	Yb	Lu
3036/9	6.91	34	72	8.5	34.	8.5	1.8	7.1	1.21	7.3	1.4	4.9	0.89	5.5	0.79
3044/16	7.69	37	81	10.3	41	9.6	1.5	9	1.34	9.4	1.8	6.1	0.82	6.6	1.02
3042/2	8.29	26	57	6.9	29.	6.7	1.2	6.2	0.88	6	1.2	3.9	0.6	4.2	0.66
3036/12	4.84	26	57	7	29.	6.4	1.6	6	0.88	5.9	1.2	3.9	0.64	3.7	0.68
1035/2	4.89	26	55	6.7	27.	6.3	1.2	6	0.88	6.2	1.3	3.9	0.54	4.2	0.63
1036/1	4.7	25	50	6	23.	5.4	1.1	4	0.6	3.8	0.8	2.6	0.44	3.1	0.5
3039/10	7.38	31	66	8	32	6.6	1.2	6.9	1.01	6.7	1.4	4.6	0.73	4.7	0.79
3039/4	6.54	30	58	7.6	29.	7.4	1.5	5.6	0.96	5.7	1.1	3.5	0.55	4	0.64
3039/20	4.2	23	48	5.9	23	4.8	1	4.1	0.55	3.6	0.8	2.3	0.37	2.5	0.4
3038/14	<0.1	3	8	1.6	9	2.7	1.3	3.7	0.63	4.2	0.9	2.8	0.37	2.2	0.34
3045/3	<0.1	5	16	2.6	13	4.4	1.5	4.4	0.67	4.7	1.1	2.9	0.4	2.8	0.4
75/1	0.78	19	44	5.9	27	6.4	2.2	7.1	1.11	6.9	1.5	4.1	0.59	4	0.54
3039/2	0.13	7	18	2.9	14	4.2	1.4	4.7	0.77	5	1.1	3.3	0.5	2.8	0.53
3038/13	0.87	14	30	4.3	18	4.4	1.1	4	0.63	3.9	0.8	2.2	0.3	1.8	0.33
3036/2	0.74	18	41	5.8	27	7	2.6	7.3	1.1	7.1	1.4	4.1	0.59	3.8	0.52
3041/1	0.71	15	35	4.6	23	5.6	1.9	6.2	0.89	6.4	1.3	3.7	0.48	3.4	0.56
3054/4	1.38	50	103	12.8	51	10.3	2.5	11.4	1.66	11.8	2.6	8.3	1.17	8.4	1.21
3054/6	1.03	51	119	14.9	62	13.5	3.9	15	2.13	14.1	2.9	8.8	1.23	8	1.09
3054/7	2.02	64	127	15.7	60	12.4	0.8	12.9	1.97	15.5	3.8	13.5	2.10	15.3	2.37
3054/2	0.89	32	72	8.7	34	7.3	2.3	7.4	1.08	7.4	1.6	4.9	0.77	5.5	0.87

detrital zircons from the southern part of the Kolyma terrane indicate an extensive tectonic event, interpreted as overthrust faulting, in the Valanginian, which happened during the main pulse of the collision of the Kolyma–Omolon superterrane with the eastern margin of the Siberian Craton [17]. The Rassokha and Argatass terranes are also located in the rear part of the Kolyma terrane. The extension deformations occurred after the intrusion of Late Jurassic granitoids in the southern part of the Main (Kolyma) Belt and the formation of the Uyandina–Yasachnaya magmatic arc [18]. $^{40}Ar/^{39}Ar$ ages from the Rassokha and Argatass terranes are 10–15 Ma younger than the zircons U–Th–Pb ages from granitoids of the Main Belt and have a Valanginian age as well [19]. It is estimated that the cooling time of granite plutons is about 10 Ma [20] and more often less. The difference between $^{40}Ar/^{39}Ar$ and U–Th–Pb dates for the part of the Main (Kolyma) Belt considered exceeds 10 Ma. It suggests that the rela-tively young $^{40}Ar/^{39}Ar$ ages, including the Valanginian dates, reflect a younger tectonic event but not the duration of cooling of granite intrusions. These data may indicate the subduction along the northeastern (in modern coordinates) part of the Kolyma–Omolon superterrane with extension in the rear part and the intrusion of subalkaline bodies, which are considered as complexes that amalgamated the Rassokha and Argatass terranes.

FUNDING

Field work and isotope–geochronological studies were carried out within the framework of the research project of FSBI VSEGEI. The isotope–geochemical data were interpreted with the support of the Russian Science Foundation (project no. 20-17-00197). Sample preparation was supported by the Russian Foundation for Basic Research (project no. 19-05-00945).

CONFLICT OF INTEREST

The authors declare that they have no conflicts of interest.

REFERENCES

1. S. D. Sokolov, Geotectonics **44** (6), 493–510 (2010).
2. V. S. Oksman, *Tectonic of Collision Cherskii Belt (North-Western Asia)* (GEOS, Moscow, 2000) [in Russian].
3. E. P. Surmilova and G. A. Maksimova, *The 1 : 200000 State Geological Map of the USSR, 3rd ed., Ser. Srednekolymskaya, Sheet No. Q-55-XXIX, XXX (Bulkut River Mouth)* (Aerogeologiya, Moscow, 1985) [in Russian].

4. M. I. Terekhov, V. M. Merzlyakov, L. A. Shpikerman, et al., *The 1 : 500000 Geological Map of the Moma, Zyryanka, Rassokha, Omulevka, Taskan, Yasachnaya, and Seimchan Rivers Heads* (Shilo North-East Interdisciplinary Sci. Res. Inst., Far East Branch RAS, Magadan, 1989) [in Russian].
5. A. P. Kropachev, A. L. Konovalov, and N. P. Fedorova, in *Stratiform Mineralization of Yakutia* (Yakutsk Division of Siberian Branch of the USSR Acad. Sci., Yakutsk, 1988), pp. 98–110 [in Russian].
6. V. I. Shpikerman, V. M. Merzlyakov, P. P. Lychagin, N. E. Savva, M. Kh. Gagiev, and V. B. Likman, Tikhookean. Geol., No. 4, 55–64 (1988).
7. I. S. Williams, Rev. Econ. Geol. **7**, 1–35 (1998).
8. L. P. Black, S. L. Kamo, C. M. Allen, J. N. Aleinikoff, D. W. Davis, R. J. Korsch, and C. Foudoulis, Chem. Geol. **200**, 155–170 (2003).
9. L. T. White and T. R. Ireland, Chem. Geol. **306–307**, 78–91 (2012).
10. J. A. Pearce, in *Continental Basalts and Mantle Xenoliths,* Ed. by C. J. Hawkesworth and M. J. Norry (Shiva Press, Natwich, 1983), pp. 230–249.
11. V. V. Akinin and E. L. Miller, Petrology **19** (3), 237–278 (2011).
12. N. V. Tsukanov and S. D. Sokolov, Russ. J. Pac. Geol. **38** (2), 99–107 (2019).
13. M. Wilson, *Igneous Petrogenesis. A Global Tectonic Approach* (Harper Collins Acad., 1991).
14. S. S. Sun and W. F. McDonough, *Chemical and Isotopic Systematics of Oceanic Basalts: Implications for Mantle Composition and Processes* (London, 1989), Vol. 42, pp. 313–345.
15. *Tectonics, Geodynamics, and Metallogeny in Sakha Republic (Yakutia),* Ed. by L. M. Parfenov and M. I. Kuz'min (Nauka, Moscow, 2001) [in Russian].
16. A. V. Rogov and S. N. Sychev, Vestn. St.-Peterb. Univ., Nauki Zemle **64** (1), 65–80 (2019).
17. A. V. Prokop'ev, V. B. Ershova, and D. Stokli, in *Proc. 51st Tectonic Meeting Problems on Continental and Ocean Tectonics* (GEOS, Moscow, 2019), pp. 141–144 [in Russian].
18. V. V. Akinin, A. V. Prokopiev, J. Toro, E. L. Miller, J. Wooden, N. A. Goryachev, A. V. Alshevsky, A. G. Bakharev, and V. A. Trunilina, Dokl. Earth Sci. **426** (4), 605–611 (2009).
19. P. W. Layer, R. Newberry, K. Fujita, L. Parfenov, V. Trunilina, and A. Bakharev, Geology **29**, 167–170 (2001).
20. T. M. Harrison, M. Grove, K. D. McKeegan, C. D. Coath, O. M. Lovera, and P. Le Fort, J. Petrol. **40**, 3–19 (1999).

Translated by D. Voroshchuk